Volume 8 | Number 5 | May 2016 | Pages 579–666

Integrative Biology

Interdisciplinary approaches for molecular and cellular life sciences

www.rsc.org/ibiology

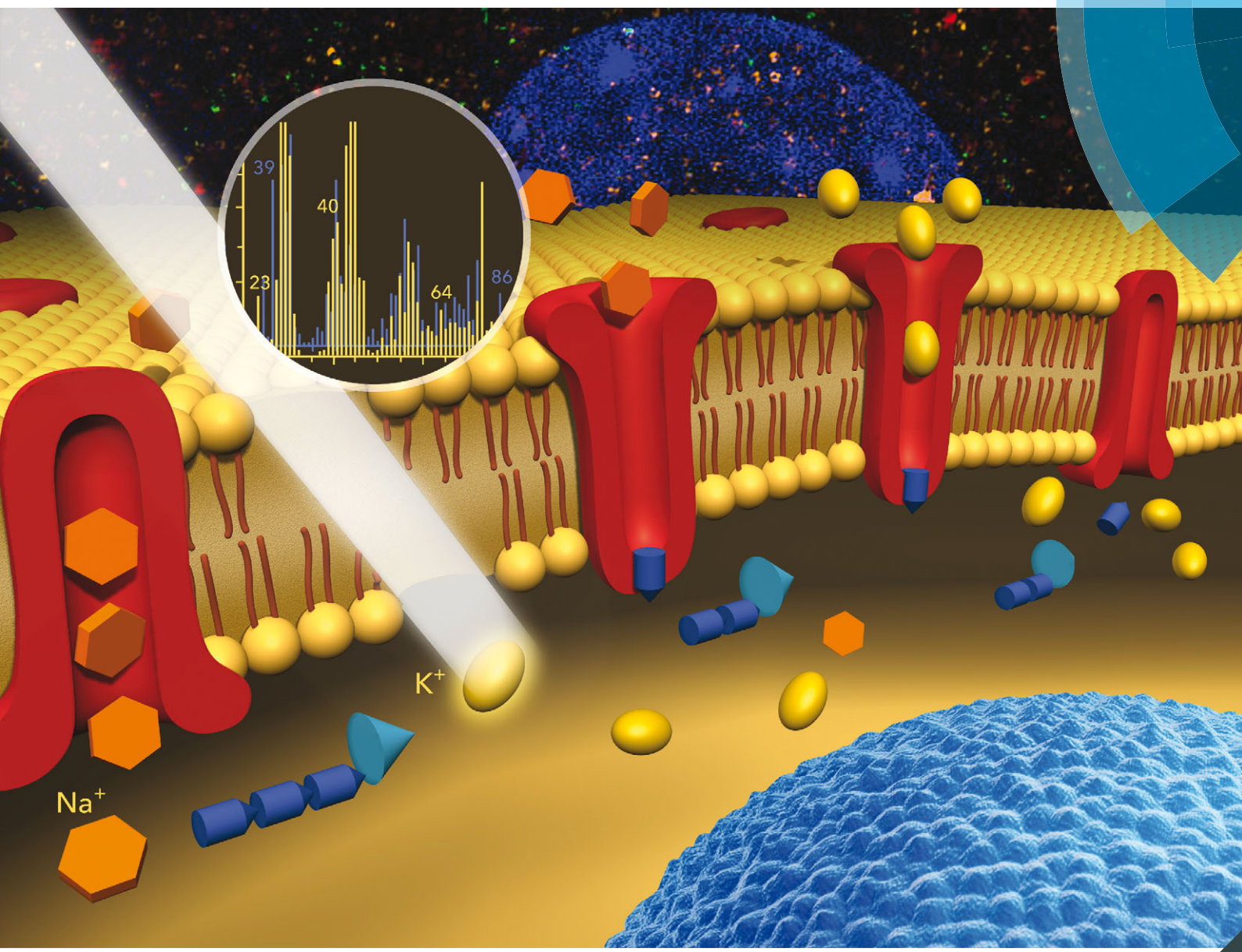

ISSN 1757-9694

ROYAL SOCIETY OF CHEMISTRY

TECHNICAL INNOVATION

Songqin Liu, Zihua Zhu, Xiao-Ying Yu *et al.*
Chemical imaging of molecular changes in a hydrated single cell by dynamic secondary ion mass spectrometry and super-resolution microscopy

Indexed in Medline!

Integrative Biology

TECHNICAL INNOVATION

Cite this: *Integr. Biol.*, 2016, 8, 635

Chemical imaging of molecular changes in a hydrated single cell by dynamic secondary ion mass spectrometry and super-resolution microscopy†

Xin Hua,[ab] Craig Szymanski,‡[c] Zhaoying Wang,‡[c] Yufan Zhou,[c] Xiang Ma,[d] Jiachao Yu,[ab] James Evans,[c] Galya Orr,[c] Songqin Liu,*[a] Zihua Zhu*[c] and Xiao-Ying Yu*[b]

Received 1st December 2015,
Accepted 18th March 2016

DOI: 10.1039/c5ib00308c

www.rsc.org/ibiology

Chemical imaging of single cells at the molecular level is important in capturing biological dynamics. Single cell correlative imaging is realized between super-resolution microscopy, namely, structured illumination microscopy (SIM), and time-of-flight secondary ion mass spectrometry (ToF-SIMS) using a multimodal microreactor (*i.e.*, System for Analysis at the Liquid Vacuum Interface, SALVI). SIM characterized cells and guided subsequent ToF-SIMS analysis. Lipid fragments were identified in the cell membrane *via* dynamic ToF-SIMS depth profiling. Positive SIMS spectra show intracellular potassium and sodium ion transport due to exposure to nanoparticles. Spectral principal component analysis elucidates differences in chemical composition among healthy alveolar epithelial mouse lung C10 cells, cells that uptake zinc oxide nanoparticles, and various wet and dry control samples. The observation of Zn^+ gives the first direct evidence of ZnO NP uptake and dissolution by the cell membrane. Our results provide submicron chemical mapping for investigating cell dynamics at the molecular level.

Insight, innovation, integration

It is a known challenge to locate molecules in an individual cell. In this work, we present the first correlative chemical imaging results using super-resolution fluorescence (*i.e.*, SIM) guided imaging mass spectrometry (*i.e.*, ToF-SIMS), and we apply this new capability to study mouse lung epithelial cells exposed to nanoparticles. Dynamic depth profiling of the cell membrane reveals first direct observations of ion transport in single cells. More importantly, this innovation has enabled surface analysis of cell membranes in a liquid, advancing our understanding of the molecular dynamics at the biomembrane interface in response to environmental stressors. The feasibility of multimodal imaging of single cells has diverse applications in systems biology, microbial ecosystems, and disease mechanisms.

Introduction

Cells, as the building block of life, have been increasingly recognized for their importance in providing insights into complex biological organization and function. Cells are not homogeneous. Cell-to-cell differences could not be captured using ensemble measurements, as subcellular chemical information may be lost. Although chemical imaging is instrumental in tracking single cells and their dynamics, locating and following moving molecules in individual cells is difficult.[1] Single cell studies, therefore, truly represent a mesoscale challenge, where interactions at multiple length scales and time scales take place.[2] Correlative imaging is considered a solution to study molecules in cellular microenvironments.[3] Collecting data at different information levels from an identical area in the same sample

[a] *School of Chemistry and Chemical Engineering, Southeast University, Nanjing, Jiangsu Province, 211189, China. E-mail: liusq@seu.edu.cn*
[b] *Earth and Biological Sciences Directorate, Pacific Northwest National Laboratory, Richland, WA 99354, USA. E-mail: xiaoying.yu@pnnl.gov*
[c] *W. R. Wiley Environmental Molecular Science Laboratory, Pacific Northwest National Laboratory, Richland, WA 99352, USA. E-mail: zihua.zhu@pnnl.gov*
[d] *Physical and Computational Sciences Directorate, Pacific Northwest National Laboratory, Richland, WA 99354, USA*

† Electronic supplementary information (ESI) available: Experimental details; schematic illustration of ToF-SIMS dynamic depth profiling; AFM measurement of the hole on the SiN membrane; ToF-SIMS depth profiling of the hydrated C10 cell in the positive and negative mode; SIMS spectral comparison among cells and control samples in both positive and negative mode; and peak assignments. See DOI: 10.1039/c5ib00308c

‡ These authors contributed equally to this work.

ideally could lead to a more holistic view of the hierarchical structural organization of cells. Thus, it potentially provides an answer to track molecules in the cell microenvironment. The cell membrane itself has a complex structure and chemical composition (*e.g.*, phospholipids, cholesterol, proteins, carbohydrates).[4] It is important in protecting a cell from the extracellular conditions, and moreover it regulates exchange of materials of its surroundings. Therefore, providing a solution to dynamically studying the liquid-like complex molecular exchange in the cell membrane could potentially address grand scientific challenges in where membrane lipids are, how they behave, and how ions are transported as a response to its surrounding microenvironment.

A number of techniques have been employed in single cell analysis including optical microscopy,[5] electron microscopy,[1] secondary ion mass spectrometry,[6] linear and non-linear vibrational spectroscopy,[7] nuclear magnetic resonance,[8] and lab-on-a chip based approaches.[9] These techniques were useful to obtain information such as cell morphology, chemical mapping, genotype, proteomics, and metabolic behaviors. Modern 3D imaging techniques introduced possibilities to expand studies at the nm scale and over various volume dimensions. Here we present first correlative imaging of single mammalian cells in their liquid microenvironment using imaging mass spectrometry, namely, time-of-flight secondary ion mass spectrometry (ToF-SIMS),[10] facilitated by super-resolution illumination fluorescence microscopy, namely structured illumination microscopy (SIM). SIM clearly images different components of a cell, *e.g.*, membrane, cytoplasm, or nucleus, whereas ToF-SIMS is a powerful tool in cell analysis including two-dimensional (2D) and three-dimensional (3D) cell imaging,[11] intracellular drug distribution mapping,[12] and cell type differentiation.[13] These two approaches also cover slightly different spatial scales. ToF-SIMS provides lateral resolution of sub-micrometers (*e.g.* <60 nm) with <1 nm resolution along the z direction. SIM is known to produce a reconstructed image with a lateral resolution twice that of diffraction-limited instruments and an axial resolution between 150 and 300 nm.

As a vacuum technique, ToF-SIMS has been traditionally limited to solid sample analysis. Biological samples are prepared using chemical fixation coupled with air drying, freeze-drying, or freeze fracture.[14] While effective in retaining the pristine cell information, the dehydration or cryogenic freezing process may alter cell component distribution or change its biological structure.[15] Therefore, methods that preserve cells in their natural microenvironment during multiplexed analyses are needed to shed new light on single cell studies.

We developed a vacuum compatible microfluidic module, System for Analysis at the Liquid Vacuum Interface (SALVI), for direct probing of liquid surfaces and interfaces by ToF-SIMS and scanning electron microscopy (SEM).[10,16] It consists of a polydimethylsiloxane (PDMS) microchannel completed by a 100 nm thick silicon nitride (SiN) membrane as the detection area. During dynamic ToF-SIMS imaging, apertures of 2 μm diameter are drilled on the SiN membrane by the bismuth (Bi) primary ion source. These apertures are used as detection windows open to vacuum, exposing the liquid directly to the primary ion beam. Because of the small aperture size, potential damage induced by evaporation and incident ions is localized. Considering the cell size, it is reasonable to expect that such a detection aperture has only limited effects on the holistic structure and function of the cell. In addition, our recent study shows that if a proper beam condition is used, the damage induced by evaporation and incident ions can be controlled in a reasonable range and molecular information can be continuously collected in the aperture.[17] In our approach, surface tension holds the liquid within the aperture. SALVI has been used to image various liquid surfaces,[18] complex solutions containing nanoparticles,[19] live biofilms,[20] or probe the solid electrode and liquid electrolyte interface.[21]

In this work, we successfully applied SALVI to study single mammalian cells, *i.e.*, alveolar type II epithelial mouse lung C10 cells, by *in situ* SIM imaging to monitor cell growth and characterize cell structure, followed by ToF-SIMS imaging to map molecules in the cell membrane. Furthermore, ToF-SIMS spectra of wet C10 cells with and without zinc oxide nanoparticle (ZnO NP) exposure were compared. The positive spectral comparison indicated intracellular potassium ion (K^+) activation by elevated calcium ions (Ca^+) after cell exposure to ZnO NPs. Spectral principal component analysis (PCA) provided further evidence of ZnO NP uptake and dissolution by the cell membrane, suggesting that dissolved Zn^+ played a critical role in inducing cytotoxicity. Our first results demonstrated SALVI as a promising tool for capturing molecular dynamics in a single cell and addressing the mesoscale challenge underpinning transient molecular interactions leading to complex cell specific functions.

Results

A schematic representationcell culturing and *in situ* SIM imaging in a 200 μm wide channel is depicted in Fig. 1a. Here the SiN window was flipped upside down, allowing cell attachment on the SiN membrane and SALVI adaptation to the SIM stage without any change. During ToF-SIMS imaging, the SiN membrane side was set to face toward the bismuth primary ion beam.[20a] A high resolution SIM image is shown in Fig. 1b, confirming the growth of C10 cells in the microchannel. To visualize cell structures with higher magnification and guide

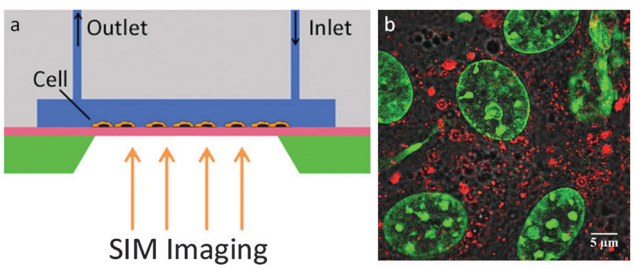

Fig. 1 Schematic illustration and SIM imaging of C10 cells in SALVI. (a) Schematic illustration of *in situ* imaging of C10 cells by SIM and SALVI. (b) High resolution SIM image overlay of bright field transmission image (grey), CdSe quantum dots (red) and DAPI (green, pseudo-color) of cultured C10 cells in the microchannel.

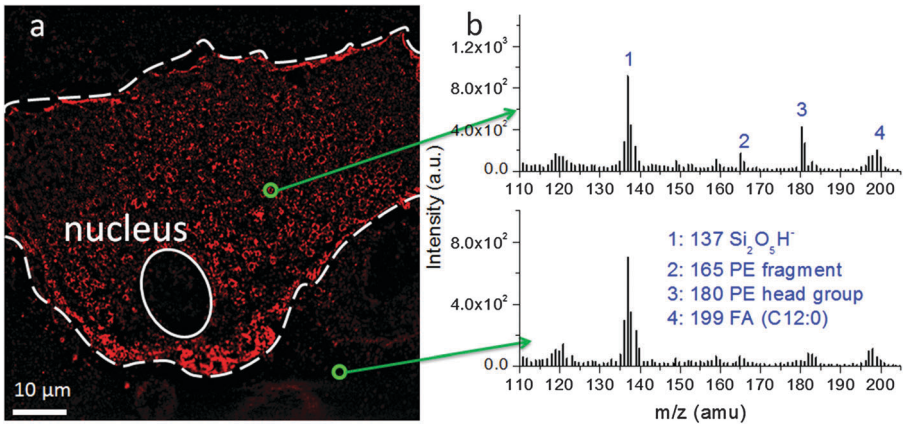

Fig. 2 Correlative imaging of C10 cells by SIM and ToF-SIMS. (a) Fluorescence SIM image of a C10 cell in SALVI. (b) ToF-SIMS negative *m/z* spectra acquired at the corresponding locations highlighted by green circles in (a).

ToF-SIMS detection, cells were exposed to uptake quantum dots. Correlative imaging of specific locations in a cell is challenging due to the relatively poor resolution of the SIMS optical microscope and incompatibility of different sample stages between SIM and ToF-SIMS. To overcome this difficulty, fluorescent microbeads were cast on the SiN surface and used as additional fiducial markers to locate regions of interest (ROIs). A fluorescence SIM image of a C10 cell is depicted in Fig. 2a. The white open circle at the bottom indicates the location of the nucleus. Quantum dots accentuated by red color illustrate the distribution of the cytoplasm. The cell membrane traced with a white dashed line has stronger illumination. Two ROIs highlighted by green circles were chosen (Fig. 2a), and ToF-SIMS spectral analyses were conducted (Fig. 2b).

An example of dynamic depth profiling in the positive ion mode is shown in Fig. 3. The reduced intensity of SiN_2^+ (*m/z* 56) indicates the SiN membrane break-through. The sharp increase of Zn^+ (*m/z* 64) provides direct evidence of ZnO NP dissolution by the cell membrane. The strong occurrence of phosphorylcholine $C_5H_{15}NO_4P^+$ (*m/z* 184) gives another confirmation of lipid components in the cell membrane. Representative peaks indicative of the liquid microenvironment (*i.e.*, $H_7O_3^+$ (*m/z* 55)) in the cell membrane are also possible using our approach. Similarly, an example of dynamic depth profiling in the negative ion mode is shown in Fig. S1 (ESI†). For example, ToF-SIMS negative spectra shown in Fig. 2b were reconstructed within 62 s after the SiN membrane punch-through in Fig. S1 (ESI†). ToF-SIMS negative spectra inside and outside the cell are different. Several representative cell fragments are observed when sampled inside the cell, such as *m/z* 165 ($C_4H_8NPO_4^-$, phosphatidylethanolamine (PE) fragment), *m/z* 180 ($C_5H_{11}NPO_4^-$, PE head group) and *m/z* 199 fatty acid ($C_{12}H_{23}O_2^-$, FA (12:0)). In contrast, these peaks have lower counts when sampled outside the C10 cell in the liquid (Fig. 2b). The *m/z* 137 peak is an interference peak from $Si_2O_5H^-$.[22]

ToF-SIMS dynamic depth profiling was performed to investigate the C10 cell chemical component variations in space and time (see Fig. S2, ESI,† for a cartoon illustration). For instance, a sharp increase in ion intensities (*e.g.*, H^- and O^-) at ~330 s

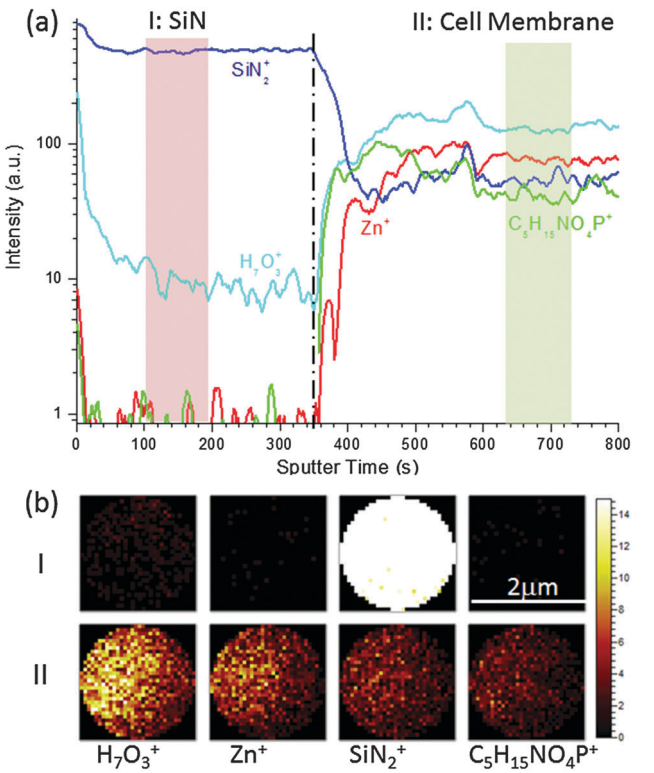

Fig. 3 ToF-SIMS depth profiling and 2D imaging of C10 cells. (a) ToF-SIMS depth profile of a hydrated C10 cell in SALVI. Two time regions indicating different depths are highlighted and defined as I (100–200 s) or before SiN punch-through and II (650–750 s) or in the cell membrane. The black dashed line indicates the beginning of SiN punch-through. (b) 2D ToF-SIMS images of $H_7O_3^+$ (*m/z* 55), SiN_2^+ (*m/z* 56), Zn^+ (*m/z* 64), and phosphorylcholine $C_5H_{15}NO_4P^+$ (*m/z* 184) reconstructed corresponding to regions I and II in (a), respectively.

(see the blue dashed line), indicative of the punch-through of the SiN membrane and the detection of water, was observed in Fig. S1 (ESI†).[16a] In addition, an increase in ion intensities of phospholipid fragments PE head group ($C_5H_{11}NPO_4^-$, *m/z* 180) and FA C12:0 (*m/z* 199) was seen. In the positive mode depth profiling, phosphatidylcholine fragments and cholesterol

fragments were observed (Fig. S3a, ESI†). These observations were postulated to be related to the punch-through of the cell membrane. Since our ToF-SIMS was not equipped with *in situ* tomography and depth measurements, additional correlative imaging with atomic force microscopy (AFM) was conducted off-line to ascertain that the SiN membrane was indeed drilled through and that cell membrane components were analyzed (Fig. S2, ESI†).

One intriguing question when using SIMS depth profiling to study water or other soft materials is the depth. In this sense, the most similar system that has been studied in the literature is the sputter yield of ice using 25 keV Au^+, Au_2^+, and Au_3^+.[23] Because the mass of Bi is similar to that of Au, we use the sputter yields of Au (*i.e.*, ~94 water molecules per 25 keV Au^+ and ~1200 water molecules per 25 keV Au_3^+) to estimate the depth profiling of water. Based on this assumption, the depth profiling rate of water in this work is estimated to be in the range of 10–30 nm s^{-1}. Given that the cell membrane is normally less than 10 nm, the cell membrane can be drilled through instantly using this rate. Water molecules as well as ions and other molecules dissolved in them can move and/or diffuse very fast in the liquid environment. Therefore a balance among evaporation, liquid diffusion, and ion bombardment can be achieved when the liquid surface is exposed in the depth profiling process.[16a,b] Unlike solids, it is difficult to sputter into liquids. As a result, a signal plateau was obtained in our depth profiling measurements.

Two time/space regions along the depth profile temporal series were highlighted and defined as region I (before SiN punch-through) and II (in the cell membrane) to illustrate 2D cell imaging (Fig. 3a). Representative 2D images were reconstructed from these time regions. The 2D spatial distributions of $H_7O_3^+$ (*m*/*z* 55), SiN_2^+ (*m*/*z* 56), Zn^+ (*m*/*z* 64), and phosphorylcholine $C_5H_{15}NO_4P^+$ (*m*/*z* 184) are illustrated in Fig. 3b. For instance, SiN_2^+ signals are higher in region I than in region II, indicating that the SiN membrane was drilled through. In contrast, $H_7O_3^+$ signals are significantly higher after the SiN punch-through in region II than in region I, indicating the observation of water clusters in the cell membrane.[16a] 2D images of characteristic fragments of the PC, *e.g.*, $C_5H_{15}NO_4P^+$ (*m*/*z* 184) and Zn^+ (*m*/*z* 64), showed a similar trend. The higher counts after the SiN membrane punch-through indicate the dynamic observation of cell components along the *z* direction corresponding to the drill-through of the cell membrane. These results demonstrated that space- and time-resolved single cell molecular mappings in the liquid microenvironment are indeed possible using SALVI enabled liquid ToF-SIMS.

In this work, because the observation window is a 2 μm diameter circle, it is not plausible to image the whole cell that is tens of micrometers at once. However, it is feasible to analyze locations of interest in a cell within the microfluidic channel once correlation between SIM and ToF-SIMS is established. Also, considering that our *in situ* liquid SIMS cannot sputter into a liquid too much due to the intrinsic mobile character of the liquid, in order to obtain interesting information in a deep location (*e.g.*, nucleus) it is prudent to develop the next generation of microfluidic devices that can accurately control or manipulate a single cell in a channel and permit SIMS analysis at any desirable locations guided by SIM or other optical techniques that can provide the picture of the whole cell.

To study cell–exogenous NP interactions, ZnO NPs were used to incubate with C10 cells. The exposure dose was determined according to Xie *et al.*[24] ToF-SIMS positive spectra are depicted in Fig. 4a. Additional negative spectra are shown in Fig. S4 (ESI†).

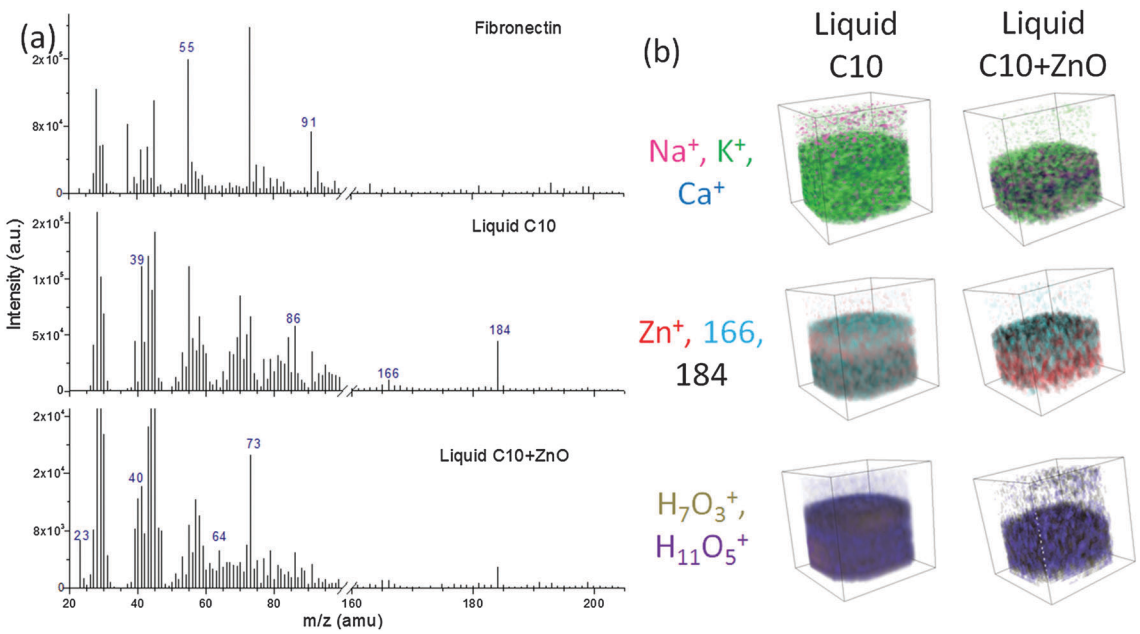

Fig. 4 (a) ToF-SIMS positive spectra of the fibronectin coated SiN–water interface, liquid C10 cells and liquid C10 cells treated with ZnO NPs in SALVI. (b) 3D images of several key *m*/*z* components of C10 and C10 cells exposed to ZnO NPs. 3D images were reconstructed from 0 to 800 s from the depth profiling time series in Fig. 3.

Peaks of water clusters (*e.g.*, *m/z* 55, 73 and 91) were found in the fibronectin coated SiN interface[25] (see Table S2, ESI,† for positive peak assignment). For liquid C10 cells, characteristic peaks of phospholipid fragments, *e.g.*, PC, were observed (*m/z* 86, 166 and 184). After treatment with ZnO nanoparticles, Zn^+ (*m/z* 64)[26] was seen in the positive spectrum, which indicated the existence of dissolved zinc ions in the cell membrane. The K^+ (*m/z* 39) and Ca^+ (*m/z* 40) intensities also differ between normal C10 cells and those exposed to ZnO NPs. The fibronectin control sample has a small *m/z* 39 peak as well. The peak *m/z* 39 may also correspond to $C_3H_3^+$. Due to the limitation of mass resolution, differentiation between K^+ and $C_3H_3^+$ is difficult in this work. Considering the relatively low background counts in the control sample, it is postulated that the larger change in the *m/z* 39 intensity between the normal C10 cell sample and the C10 cells exposed to ZnO NPs may mainly arise from the K^+ ion channel activation. After a high dose exposure of ZnO NPs, the Ca^+ counts were much higher than K^+ counts, indicating decreased intracellular K^+. Interestingly, the *m/z* 23 (Na^+) count is higher in the membrane of C10 cells exposed to ZnO NPs compared to the normal C10 cells.

Reconstructed 3D images of representative peaks from 0 to 800 s along the depth profiling time series in Fig. 3 are depicted in Fig. 4b. The 3D visualization showed ZnO NP dissolution by the cell membrane more vividly after the C10 cell exposure, as the Zn^+ was more densely located deeper in the cell membrane. Similarly, the C10 cells exposed to ZnO NP seemed to have more reduced K^+ yet elevated Ca^+ and Na^+ in the cell membrane. This observation provides additional evidence of intracellular ion transport through the membrane ion channel after the cell experiences oxidative stress that affects the epithelial sodium channel activities.[27]

Spectral PCA was performed to obtain a better understanding of cell molecular component differences among samples in the positive mode. All peaks in the *m/z* range 20–200 were used in the analysis. The PCA score plot of the first two principal components (PCs), namely, PC1 and PC2, is depicted in Fig. 5a. PC1 and PC2 captured 76.6% of the variance. Clear discriminations among control samples (DI water and fibronectin coated SiN–water interface), hydrated C10 cells, ZnO NP exposed C10 cells, ZnO NPs, and dried C10 cells were observed. The loading plots of PC1 and PC2 (Fig. 5b) showed key contributors for the observed similarities and differences.

Dry C10 cells, liquid C10 cells, and C10 cells exposed to ZnO NPs are separated by PC1. Peaks such as *m/z* 23 (Na^+), 39 (K^+), 55 ($(H_2O)_3H^+$), 70 ($C_4H_8N^+$, proline fragment), 91 ($(H_2O)_5H^+$), or 184 ($C_5H_{15}NO_4P^+$, phosphatidylcholine fragment) are key contributors for separating dry and wet C10 cells. In contrast, peaks including *m/z* 40 (Ca^+), 45, 57, 64 (Zn^+), or 73 ($(H_2O)_4H^+$ or PDMS interference $SiC_3H_9^+$) are more typical of C10 cells exposed to ZnO NPs. Ca^+ is more dominant in C10 cells exposed to ZnO NPs, whereas Na^+ and K^+ are more significant in the normal C10 cells. In addition, Zn^+ (*m/z* 64) is one of the key peaks that differentiate ZnO NP treated cells and normal C10 cells, indicating that dissolved ZnO NPs were observed in the cell membrane.[28] The peak *m/z* 45 has been observed in the

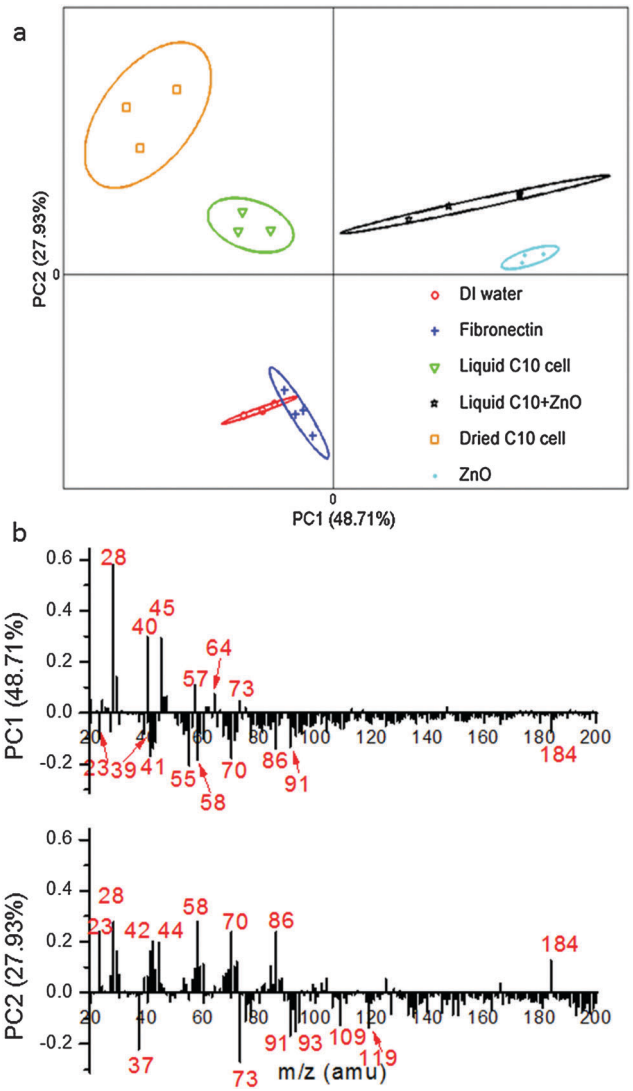

Fig. 5 PCA results for different samples. (a) The PCA score plot of DI water, fibronectin coated SiN–water interface, liquid C10 cells cultured in SALVI, liquid C10 cells treated with ZnO in SALVI, ZnO NPs in SLAVI, and dried C10 cells on the SiN membrane. An ellipse defining 95% confidence limit of each sample type is shown in the same color corresponding to each sample cluster. (b) PC1 and PC2 loading plots showing the *m/z* responsible for the separation.

SIMS spectra of model cell membranes using glycophospholipids, cholesterol, and glycophorin.[29] It can be assigned to multiple species, such as $C_2H_5O^+$,[30] CO_2H^+, or $SiOH^+$,[31] when using the unit mass peak resolution. Peak assignment from the interference peak $SiOH^+$ is likely because of the usage of PDMS and SiN to construct the microchannel; however contributions from $C_2H_5O^+$ and CO_2H^+ are also possible. The identity of *m/z* 57 is inconclusive. It may arise from unsaturated fragment ions produced during ZnO NP synthesis.[32] These results also provide molecular evidence that dissolved Zn^+ ions from ZnO NPs are important in inducing the oxidative stress through cell membrane processes.[33]

PC2 separates the two wet control samples, DI water and the fibronectin coated SiN membrane, and the rest of the dry or wet

C10 samples. The peaks that contribute mainly to this separation are mostly water clusters in the PC2 negative space, including m/z 37 ($(H_2O)_2H^+$), 73 ($(H_2O)_4H^+$), 91 ($(H_2O)_5H^+$), 109 ($(H_2O)_6H^+$), or 119 ($(H_2O)_7H^+$). This is reasonable as these two control samples have characteristic water clusters.[25] In contrast, samples residing in the PC2 positive side all share characteristics of cell membranes such as m/z 58 ($C_3H_8N^+$), 86 ($C_5H_{12}N^+$), 166 ($C_5H_{13}NO_3P^+$), and 184 ($C_5H_{15}NO_4P^+$). They are all phosphatidylcholine fragment peaks. This is expected because these samples have cell components. The PCA results demonstrate that SALVI and ToF-SIMS can provide new insights into chemical differences of cell membrane components in the liquid microenvironment.

Discussion

A main challenge to study single cells using vacuum-based surface techniques such as imaging mass spectrometry (*i.e.*, ToF-SIMS) and electron microscopy (*e.g.*, SEM) lies in introducing a biologically viable sample in its native liquid environment without altering or modifying it during sample preparation and subsequent analysis. It is known that air- or freeze-drying may result in sample changes.[34] New methods that permit direct observation of single cells in their liquid environment are needed. We report the first correlative bioimaging of hydrated single mammalian cells by super-resolution fluorescence microscopy (*i.e.*, SIM), imaging mass spectrometry (*i.e.*, ToF-SIMS), and AFM using SALVI, a multimodal vacuum compatible microreactor. More effective correlative imaging can be facilitated by making transferrable sample stages among different instruments.

More importantly, the unique capability to observe wet cell chemical distribution in the cell membrane in their liquid microenvironment allows us to potentially study apoptotic cell death, cell proliferation, or cytotoxicity with both ionic and molecular insight. The identification of Zn^+ (m/z 64) as dissolved ions from ZnO NPs was also reported by Lee *et al.* in a cytotoxicity study of ZnO NPs using dry human keratinocytes (HaCaT).[28b] Although the Ga^+ primary ion beam was used in this earlier study, it is expected that the ionization efficiency of Bi_3^+ primary ion beams would also result in Zn^+ from ZnO NPs.[35] In this earlier ToF-SIMS study, human HaCaT cells were exposed to ZnO NPs and dried before further analysis. A decreased intracellular K^+ (m/z 39) level was observed and it was speculated that it was a result of the K^+ channel activated by elevated Ca^+ (m/z 40). It was hypothesized that dissolved Zn^+ ions (m/z 64) from ZnO NPs might have played a critical role in inducing cytotoxicity.[28b] In our observations in the positive spectra, the Ca^+ counts are much higher than K^+ counts after a high dose exposure of ZnO NPs (Fig. 4), indicating decreased intracellular K^+ in the cell membrane in the hydrated state. The observation of epithelial sodium channel activity is also seen in the SIMS spectra of the mouse alveolar type II cell membrane. Since the microfluidic channel was rinsed using DI water to reduce the sodium signals from the PBS buffer after cells were fixed, the subtle change in Na^+ was more likely to be observed. The observation of ion changes in the nanometer thick cell membrane in the hydrated state potentially provides the first direct evidence of sodium and potassium transport in the ion channel in the alveolar epithelial cell membrane[36] and the importance of the ion channel in cell functions[37,38] at the molecular level elucidated by multiplexed *in situ* chemical imaging.

We envision that continued development in microfluidic reactor design would facilitate cell manipulation in a well-defined microenvironment, permitting single cell optical imaging coupled with advanced SIMS imaging. One direction, for example, may involve 3D cell cultures that allow more complex cell types to be studied in the liquid state using *in situ* molecular mapping offered by imaging mass spectrometry. It is equally important to advance SIMS as an analytical technique, for instance, increasing ion yields, mass resolution, and spatial resolution, simultaneously. Several new instruments are on the horizon to address these kinds of technical challenges. One representative example is the J105 from Ionoptika;[39] the other is the addition of an Orbitrap to an existing commercial IONTOF ToF-SIMS instrument *via* collaboration among NPL, IONTOF, and Thermo Fisher.[40] Ideally, coupling our microfluidic interface with these types of novel SIMS capabilities will provide high spatial resolution and high mass resolution measurements simultaneously in the future.

Methods

SALVI fabrication

The fabrication process was described in our earlier papers.[10,16a,b] Briefly, soft lithography was employed to make a 200 μm wide by 300 μm deep channel on a PDMS block. A SiN window consisting of a 100 nm thick SiN membrane and a silicon frame (frame size 7.5 × 7.5 mm^2, window size 1.5 × 1.5 mm^2, Norcada, Edmonton, Canada) was bonded to the PDMS block by oxygen plasma treatment. The two pieces are brought to each other by immediate contact to seal the microchannel and form the detection area.

Cell culturing and dried sample preparation

For dried sample preparation, C10 cells were seeded onto an individual silicon-framed, fibronectin-coated (Catalog number F1141, Sigma-Aldrich) SiN membrane at a density of 10^5 cells per mL. These cells were cultured in RPMI 1640 medium (Gibco, Grand Island, NY, USA) supplemented with 10% fetal bovine serum (Gibco, Grand Island, NY, USA) for 48 hours at 37 °C in a humidified atmosphere containing 5% CO_2. To remove the salts on the cell, which may greatly lower the organic secondary ion yield of the biological sample,[41] 150 mM ammonium acetate (Sigma-Aldrich, Saint Louis, MO, USA) solution was used to rinse the cells on the SiN membrane. After that, cells were placed into a 4% paraformaldehyde (Electron Microscopy Sciences, Hatfield, PA, USA) solution for 30 min for fixation. Finally, cells were rinsed with DI water and allowed to air dry overnight in a laminar flow hood.[14]

Cell culturing in SALVI

The microchannel in SALVI was thoroughly washed with 70% ethanol and sterilized DI water, and then treated with 10 mg mL^{-1} fibronectin solution overnight. Then 500 μL of C10 cell suspension (10^6 cells per mL) was injected into the channel, followed by incubation at 37 °C for 24 h in a humidified atmosphere containing 5% CO_2. Fresh medium was passed through the channel before a subsequent cell culturing for 48 h. Carboxylate-functionalized CaSe quantum dots (655 nm emission, Catalog number: Q21321MP, Thermo Fisher, Carlsbad, CA, USA) dispersed in cell culture medium with a concentration of 5 nM were flown through the channel for 24 h. Quantum dots were chosen for their extraordinary photostability and labeling of the cell cytoplasm. The cultured cells were washed with PBS, fixed with 4% paraformaldehyde and stained with DAPI (Catalog number: D1306, Life Technologies). In order to reduce the background signals from the PBS buffer in ToF-SIMS analysis, DI water was used to wash the channel after cells were fixed and treated with stains before SIM imaging and subsequent ToF-SIMS analysis.

SIM imaging

SIM Imaging was performed on an Elyra S1 inverted fluorescence microscope (Zeiss, Jena, Germany). An oil immersion objective with 63× magnification and 1.4 numerical aperture was used in this study. 5 rotations and 5 phases were taken for each SIM image. The pixel size in the raw images was 80 nm per pixel, and in the resulting super-resolution images it was 40 nm per pixel. The camera exposure time was 100 ms per image. The excitation source was a 405 nm laser with 9 mW power and emission was collected at 655 nm and above. Bright field transmission images were also collected at conventional resolution. SIM images were processed to provide super-resolution images using ZEN software (Zeiss, Jena, Germany).

ToF-SIMS imaging

A ToF-SIMS V spectrometer (IONTOF GmbH, Münster, Germany) was used in this study. The analytical capability of SALVI enabled liquid ToF-SIMS was detailed in our earlier paper.[19] Potential interference from liquid diffusion after punching-through in SIMS measurements may not be as significant as those cases of aqueous solutions.[16b,21] In the SIM and ToF-SIMS correlative imaging study, a 25 keV Bi^+ beam was used as the primary ion beam. In order to capture the organic components better, a pulsed 25 keV Bi_3^+ primary ion beam was also used. During SIM and SIMS correlative measurements, the Bi^+ beam was focused to about ~250 nm diameter, and it was scanned on a round area with a diameter of ~2 μm. To save the punch-through time of the SiN film, a long pulse-width (1000 ns, beam current ~7.7 pA at a repeated frequency of 20 kHz) Bi^+ beam was used for pre-punching for ~115 s, and then the pulse width was reduced to 130 ns for data collection (beam current ~1.0 pA at a repeated frequency of 20 kHz). When the Bi_3^+ primary ion beam was used, it was focused to about 450 nm diameter with a beam current of ~0.36 pA (10 kHz). A pulse width of ~150 ns was used for sputtering through the SiN membrane, and then the pulse width was changed to 50 ns to obtain a better mass resolution. Vacuum pressure during measurements was 2.5–5.5 × 10^{-7} mbar in the analysis chamber, indicating that no spraying or fast spreading of aqueous solutions from the aperture occurred.[16a] Before each measurement, a 500 eV O_2^+ beam (~40 nA) was scanned on the SiN window with a 400 × 400 μm^2 area for ~30 s to remove surface contamination. Also, an electron flood gun was used to compensate surface charging during all measurements. All data were analyzed using the IONTOF software (SurfaceLab, version 6.3). Mass spectra were calibrated using C^+, CH^+, CH_2^+ and Na^+ peaks in the positive spectra, and C^-, CH^-, CH_2^-, O^-, OH^- and PO_2^- peaks in the negative spectra, respectively.[42] For spectral PCA, unit mass peaks within m/z 20–200 were used, and MATLAB R2012a (MathWorks, Natick, MA, USA) was used for the analysis.[42]

AFM imaging

AFM imaging was performed in air using an MFP-3D AFM (Asylum Research) instrument at room temperature. Silicon cantilevers (SSS-NCL, NanoWorld) with a tip radius of <5 nm and a spring constant of ~48 N m^{-1} were used. AFM images were obtained in the tapping mode using low set point amplitudes (<300 mV) to minimize damage to samples. Images were analyzed using Igor Pro 6.34 software (WaveMetrics).

Correlative imaging among SIM, ToF-SIMS, and AFM

To facilitate correlative imaging between ToF-SIMS, SIM, and AFM, different shapes of markers were made by the ToF-SIMS primary ion beam along the microchannel corresponding to different apertures drilled in the dynamic ToF-SIMS analysis. These markers were imaged using the ToF-SIMS microscope and other light microscopes. The photos were used as references when bringing the same cell sample to the AFM for correlation and finding the exact location along the channel.

For correlation of SIM with ToF-SIMS, images were collected for the entire 1.5 × 1.5 mm^2 sample area using conventional bright field imaging before and after ToF-SIMS imaging. Additional fiducial markers along the microchannel were used to help collocation. The holes in the membrane from ToF-SIMS analysis were clearly visible in the bright field images, allowing matching of ToF-SIMS spectra with specific locations in SIM fluorescence images. Correlated images were overlaid using the MATLAB Image Processing Toolbox (MathWorks, Natick, MA, USA).

Nanoparticle toxicity

Aerosolized zinc oxide (ZnO) nanoparticles (NPs) are known to induce toxicity in alveolar type II epithelial cells (C10). ZnO NPs (US 3599) were purchased from US Research Nanomaterials, Inc. The detailed characterization of ZnO NPs is described in an earlier paper.[24] The average particle size is 18 nm. According to Xie *et al.*,[24] a significant oxidative stress was detected in response to a high dose (*i.e.*, 100 μg mL^{-1}) of aerosolized ZnO NPs at 6 h post-exposure. This was the dose used in this study. The dose was also cross-calibrated using the standard curve reported in Mihai *et al.*[33b]

Conclusions

The first dynamic molecular spatial mapping by ToF-SIMS correlated with SIM illustrated submicrometer chemical molecular distribution in a single cell. Spectral PCA results provided molecular differences among cells with and without exposure to toxic nanoparticles. This unique approach potentially provides a new tool to study single cell nanoparticle toxicity at both ionic and molecular level in liquids. These results demonstrate that the single cell biointerphase at the nanometer scale can be studied dynamically. This work illustrates the importance of multiplexed imaging to capture molecular changes in cells in their liquid microenvironment. The multimodality enabled by SALVI will open a new door for imaging and investigating complex dynamics at the molecular level and linking cellular processes occurring at the mesoscale.

Author contributions

X. H., C. S., Z. W., Y. Z., X. M., and J. Y. conducted the experiments. X. H., C. S., and X.-Y. Y. analyzed the data. J. E. and G. O. provided the samples. G. O., S. L., and Z. Z. provided technical guidance. X.-Y. Y., X. H., Z. Z., C. S., and X. M. prepared the manuscript. X.-Y. Y. supervised the project.

Acknowledgements

We are grateful for the support from the Pacific Northwest National Laboratory (PNNL) Chemical Imaging Initiative (CII) Laboratory Directed Research and Development (LDRD) and Earth and Biological Sciences Directorate (EBSD) mission seed LDRD Fund. The research was performed in the W. R. Wiley Environmental Molecular Sciences Laboratory, a national scientific user facility sponsored by OBER and located at PNNL. PNNL is operated for DOE by Battelle.

Notes and references

1 K. Galler, K. Brautigam, C. Große, J. Popp and U. Neugebauer, Making a big thing of a small cell – recent advances in single cell analysis, *Analyst*, 2014, **139**, 1237–1273, DOI: 10.1039/c3an01939j.

2 R. Masyuko, E. J. Lanni, J. V. Sweedler and P. W. Bohn, Correlated imaging – a grand challenge in chemical analysis, *Analyst*, 2013, **138**, 1924–1939, DOI: 10.1039/c3an36416j.

3 B. P. Cinquin, M. Do, G. McDermott, A. D. Walters, M. Myllys, E. A. Smith, O. Cohen-Fix, M. A. Le Gros and C. A. Larabell, Putting Molecules in Their Place, *J. Cell. Biochem.*, 2014, **115**, 209–216, DOI: 10.1002/jcb.24658.

4 (*a*) G. L. Nicolson, The fluid—mosaic model of membrane structure: still relevant to understanding the structure, function and dynamics of biological membranes after more than 40 years, *Biochim. Biophys. Acta, Biomembr.*, 2014, **1838**, 1451–1466, DOI: 10.1016/j.bbamem.2013.10.019; (*b*) G. van Meer, D. R. Voelker and G. W. Feigenson, Membrane lipids: where they are and how they behave, *Nat. Rev. Mol. Cell Biol.*, 2008, **9**, 112–124.

5 T. Arnold, K. Grossmann and N. Baumann, Uranium speciation in biofilms studied by laser fluorescence techniques, *Anal. Bioanal. Chem.*, 2010, **396**, 1641–1653, DOI: 10.1007/s00216-009-3296-5.

6 C. Szakal, K. Narayan, J. Fu, J. Lefman and S. Subramaniam, Compositional Mapping of the Surface and Interior of Mammalian Cells at Submicrometer Resolution, *Anal. Chem.*, 2011, **83**, 1207–1213, DOI: 10.1021/ac1030607.

7 H. J. van Manen, Y. M. Kraan, D. Roos and C. Otto, Single-cell Raman and fluorescence microscopy reveal the association of lipid bodies with phagosomes in leukocytes, *Proc. Natl. Acad. Sci. U. S. A.*, 2005, **102**, 10159–10164, DOI: 10.1073/pnas.0502746102.

8 S. J. DeVience, L. M. Pham, I. Lovchinsky, A. O. Sushkov, N. Bar-Gill, C. Belthangady, F. Casola, M. Corbett, H. L. Zhang, M. Lukin, H. Park, A. Yacoby and R. L. Walsworth, Nanoscale NMR spectroscopy and imaging of multiple nuclear species, *Nat. Nanotechnol.*, 2015, **10**, 129–134, DOI: 10.1038/nnano.2014.313.

9 H. N. Joensson and H. A. Svahn, Droplet Microfluidics-A Tool for Single-Cell Analysis, *Angew. Chem., Int. Ed.*, 2012, **51**, 12176–12192, DOI: 10.1002/anie.201200460.

10 X.-Y. Yu, L. Yang, J. Cowin, M. Iedema and Z. Zhu, *US Pat.*, 8555710 B2, 2013.

11 M. A. Robinson, D. J. Graham and D. G. Castner, ToF-SIMS Depth Profiling of Cells: z-Correction, 3D Imaging, and Sputter Rate of Individual NIH/3T3 Fibroblasts, *Anal. Chem.*, 2012, **84**, 4880–4885, DOI: 10.1021/ac300480g.

12 P. Sjövall, T. M. Greve, S. K. Clausen, K. Moller, S. Eirefelt, B. Johansson and K. T. Nielsen, Imaging of Distribution of Topically Applied Drug Molecules in Mouse Skin by Combination of Time-of-Flight Secondary Ion Mass Spectrometry and Scanning Electron Microscopy, *Anal. Chem.*, 2014, **86**, 3443–3452, DOI: 10.1021/ac403924w.

13 J. F. Frisz, J. S. Choi, R. L. Wilson, B. A. C. Harley and M. L. Kraft, Identifying Differentiation Stage of Individual Primary Hematopoietic Cells from Mouse Bone Marrow by Multivariate Analysis of TOF-Secondary Ion Mass Spectrometry Data, *Anal. Chem.*, 2012, **84**, 4307–4313, DOI: 10.1021/ac203329j.

14 M. A. Robinson and D. G. Castner, Characterization of sample preparation methods of NIH/3T3 fibroblasts for ToF-SIMS analysis, *Biointerphases*, 2013, **8**, 15, DOI: 10.1186/1559-4106-8-15.

15 A. C. Dohnalkova, M. J. Marshall, B. W. Arey, K. H. Williams, E. C. Buck and J. K. Fredrickson, Imaging Hydrated Microbial Extracellular Polymers: Comparative Analysis by Electron Microscopy, *Appl. Environ. Microbiol.*, 2011, **77**, 1254–1262, DOI: 10.1128/AEM.02001-10.

16 (*a*) L. Yang, X.-Y. Yu, Z. Zhu, M. J. Iedema and J. P. Cowin, Probing liquid surfaces under vacuum using SEM and ToF-SIMS, *Lab Chip*, 2011, **11**, 2481–2484; (*b*) L. Yang, X.-Y. Yu, Z. H. Zhu, T. Thevuthasan and J. P. Cowin, Making a hybrid microfluidic platform compatible for *in situ* imaging by vacuum-based techniques, *J. Vac. Sci. Technol., A*, 2011,

29, 061101, DOI: 10.1116/1.3654147; (*c*) X.-Y. Yu, L. Yang, Z. H. Zhu, J. P. Cowin and M. J. Iedema, Probing aqueous surfaces by ToF-SIMS, *Spectroscopy: Current Trends in Mass Spectrometry*, 2011, **2011**(supplemental), 34–38.

17 Y. Zhou, Y. Ding, J. Yu, X. Hua, J. Evans, X. Yu, D. Lao, X. Wang, X.-Y. Yu and Z. Zhu, Can *in situ* liquid SIMS provide enough signals for biological and environmental research?, *J. Mass Spectrom.*, 2016, submitted.

18 L. Yang, Z. Zhu, X.-Y. Yu, S. Thevuthasan and J. P. Cowin, Performance of a microfluidic device for *in situ* ToF-SIMS analysis of selected organic molecules at aqueous surfaces, *Anal. Methods*, 2013, **5**, 2515–2522, DOI: 10.1039/c3ay26513g.

19 L. Yang, Z. Zhu, X.-Y. Yu, E. Rodek, L. Saraf, T. Thevuthasan and J. P. Cowin, *In situ* SEM and ToF-SIMS analysis of IgG conjugated gold nanoparticles at aqueous surfaces, *Surf. Interface Anal.*, 2014, 224–228, DOI: 10.1002/sia.5252.

20 (*a*) X. Hua, X.-Y. Yu, Z. Wang, L. Yang, B. Liu, Z. Zhu, A. E. Tucker, W. B. Chrisler, E. A. Hill, T. Thevuthasan, Y. Lin, S. Liu and M. J. Marshall, *In situ* molecular imaging of hydrated biofilm in a microfluidic reactor by ToF-SIMS, *Analyst*, 2014, **139**, 1609–1613; (*b*) X. Hua, M. J. Marshall, Y. Xiong, X. Ma, Y. Zhou, A. E. Tucker, Z. Zhu, S. Liu and X.-Y. Yu, Two-dimensional and three-dimensional dynamic imaging of live biofilms in a microchannel by time-of-flight secondary ion mass spectrometry, *Biomicrofluidics*, 2015, **9**, 031101, DOI: 10.1063/1.4919807.

21 B. Liu, X.-Y. Yu, Z. Zhu, X. Hua, L. Yang and Z. Wang, *In situ* chemical probing of the electrode–electrolyte interface by ToF-SIMS. Lab Chip, 2014, **14**, 855–859, DOI: 10.1039/c3lc50971k.

22 G. S. Groenewold, J. R. Scott, A. K. Gianotto, B. D. M. Hodges, G. F. Kessinger, M. T. Benson and J. B. Wright, Gas-Phase Condensation Reactions of SixOyHz-Oxyanions with H_2O, *J. Phys. Chem. A*, 2001, **105**, 9681–9688, DOI: 10.1021/jp010905e.

23 (*a*) C. Szakal, J. Kozole and N. Winograd, Fundamental studies of the cluster ion bombardment of water ice, *Appl. Surf. Sci.*, 2006, **252**, 6526–6528, DOI: 10.1016/j.apsusc.2006.02.208; (*b*) C. Szakal, J. Kozole, M. F. Russo, B. J. Garrison and N. Winograd, Surface sensitivity in cluster-ion-induced sputtering, *Phys. Rev. Lett.*, 2006, **96**, 216104, DOI: 10.1103/Physrevlett.96.216104.

24 Y. Xie, N. G. Williams, A. Tolic, W. B. Chrisler, J. G. Teeguarden, B. L. S. Maddux, J. G. Pounds, A. Laskin and G. Orr, Aerosolized ZnO Nanoparticles Induce Toxicity in Alveolar Type II Epithelial Cells at the Air–Liquid Interface, *Toxicol. Sci.*, 2012, **125**, 450–461, DOI: 10.1093/toxsci/kfr251.

25 J. Yu, Y. Zhou, X. Hua, Z. Zhu and X.-Y. Yu, *In situ* characterization of hydrated proteins in water by SALVI and ToF-SIMS, *J. Visualized Exp.*, 2016, **108**, e53708, DOI: 10.3791/53708.

26 (*a*) M. J. Stein, E. Lo, D. G. Castner and B. D. Ratner, Plasma Pencil Atmospheric Mass Spectrometry Detection of Positive Ions from Micronutrients Emitted from Surfaces, *Anal. Chem.*, 2012, **84**, 1572–1578, DOI: 10.1021/ac2028134; (*b*) A. V. Ghule, K. Ghule, C.-Y. Chen, W.-Y. Chen, S.-H. Tzing, H. Chang and Y.-C. Ling, *In situ* thermo-TOF-SIMS study of thermal decomposition of zinc acetate dihydrate. Journal of Mass Spectrometry, 2004, **39**, 1202–1208, DOI: 10.1002/jms.721.

27 C. Planès, B. Escoubet, M. Blot-Chabaud, G. Friedlander, N. Farman and C. Clerici, Hypoxia Downregulates Expression and Activity of Epithelial Sodium Channels in Rat Alveolar Epithelial Cells, *Am. J. Respir. Cell Mol. Biol.*, 1997, **17**, 508–518, DOI: 10.1165/ajrcmb.17.4.2680.

28 (*a*) K. Ghule, A. V. Ghule, B.-J. Chen and Y.-C. Ling, Preparation and characterization of ZnO nanoparticles coated paper and its antibacterial activity study, *Green Chem.*, 2006, **8**, 1034–1041, DOI: 10.1039/B605623G; (*b*) P.-L. Lee, S.-Y. Shen and Y.-S. Yin, Invited paper: ToF-SIMS imaging of intracellular 39K/40Ca changes induced by ZnO-containing nanomaterials (Proceedings of the 5th international symposium on practical surface analysis PSA-10 and 7th Korea–Japan international symposium on surface analysis), *J. Surf. Anal.*, 2011, **17**, 305–309.

29 M. J. Baker, L. Zheng, N. Winograd, N. P. Lockyer and J. C. Vickerman, Mass Spectral Imaging of Glycophospholipids, Cholesterol, and Glycophorin A in Model Cell Membranes, *Langmuir*, 2008, **24**, 11803–11810, DOI: 10.1021/la802582f.

30 N. Médard, M. Aouinti, F. Poncin-Epaillard and P. Bertrand, ToF-SIMS ability to quantify surface chemical groups: correlation with XPS analysis and spectrochemical titration, *Surf. Interface Anal.*, 2001, **31**, 1042–1047, DOI: 10.1002/sia.1138.

31 M. C. Perkins, G. Bell, D. Briggs, M. C. Davies, A. Friedman, C. A. Hart, C. J. Roberts and F. J. M. Rutten, The application of ToF-SIMS to the analysis of herbicide formulation penetration into and through leaf cuticles, *Colloids Surf., B*, 2008, **67**, 1–13, DOI: 10.1016/j.colsurfb.2008.04.019.

32 A. Kołodziejczak-Radzimska and T. Jesionowski, Zinc Oxide—From Synthesis to Application: A Review, *Materials*, 2014, **7**, 2833.

33 (*a*) T. Xia, M. Kovochich, M. Liong, L. Mädler, B. Gilbert, H. Shi, J. I. Yeh, J. I. Zink and A. E. Nel, Comparison of the Mechanism of Toxicity of Zinc Oxide and Cerium Oxide Nanoparticles Based on Dissolution and Oxidative Stress Properties, *ACS Nano*, 2008, **2**, 2121–2134, DOI: 10.1021/nn800511k; (*b*) C. Mihai, W. B. Chrisler, Y. Xie, D. Hu, C. J. Szymanski, A. Tolic, J. A. Klein, J. N. Smith, B. J. Tarasevich and G. Orr, Intracellular accumulation dynamics and fate of zinc ions in alveolar epithelial cells exposed to airborne ZnO nanoparticles at the air–liquid interface, *Nanotoxicology*, 2015, **9**, 9–22, DOI: 10.3109/17435390.2013.859319.

34 M. Wojcik, M. Hauser, W. Li, S. Moon and K. Xu, Graphene-enabled electron microscopy and correlated super-resolution microscopy of wet cells, *Nat. Commun.*, 2015, **6**, 7384, DOI: 10.1038/ncomms8384.

35 J. C. Vickerman and D. Briggs, *ToF-SIMS Surface Analysis by Mass Spectrometry*, IM Publications LLP, 2nd edn, 2013, p. 586.

36 S. Matalon and H. O'Brodovich, Sodium Channels in Alveolar Epithelial Cells: Molecular Characterization, Biophysical Properties, and Physiological Significance, *Annu. Rev. Physiol.*, 1999, **61**, 627–661, DOI: 10.1146/annurev.physiol.61.1.627.

37 F. Lang, M. Föller, K. S. Lang, P. A. Lang, M. Ritter, E. Gulbins, A. Vereninov and S. M. Huber, Ion Channels in Cell Proliferation and Apoptotic Cell Death, *J. Membr. Biol.*, 2005, **205**, 147–157, DOI: 10.1007/s00232-005-0780-5.

38 K. Kunzelmann, Ion Channels and Cancer, *J. Membr. Biol.*, 2005, **205**, 159–173, DOI: 10.1007/s00232-005-0781-4.

39 S. Rabbani, J. S. Fletcher, N. P. Lockyer and J. C. Vickerman, Exploring subcellular imaging on the buncher-ToF J105 3D chemical imager, *Surf. Interface Anal.*, 2011, **43**, 380–384, DOI: 10.1002/sia.3457.

40 (*a*) NPL, 3D nanoSIMS – label-free molecular imaging, 2013, http://www.npl.co.uk/news/3d-nanosims-label-free-molecular-imaging; (*b*) IONTOF, A new revolutionary companion for the TOF.SIMS 5, 2015, https://www.iontof.com/news-ion-tof-sims-events.html.

41 A. M. Piwowar, N. P. Lockyer and J. C. Vickerman, Salt Effects on Ion Formation in Desorption Mass Spectrometry: An Investigation into the Role of Alkali Chlorides on Peak Suppression in Time-of-Flight-Secondary Ion Mass Spectrometry, *Anal. Chem.*, 2009, **81**, 1040–1048, DOI: 10.1021/ac8020888.

42 F. M. Green, I. S. Gilmore and M. P. Seah, TOF-SIMS: Accurate mass scale calibration, *J. Am. Soc. Mass Spectrom.*, 2006, **17**, 514–523, DOI: 10.1016/j.jasms.2005.12.005.

